nature chemical biology

Article

https://doi.org/10.1038/s41589-024-01713-2

Degradable living plastics programmed by engineered spores

Received: 15 March 2023

Accepted: 29 July 2024

Published online: 21 August 2024

Check for updates

Chenwang Tang[1,2], Lin Wang[1,6], Jing Sun[2,3,6], Guangda Chen[4], Junfeng Shen[1], Liang Wang[5], Ying Han[1], Jiren Luo[1], Zhiying Li[5], Pei Zhang[4], Simin Zeng[1], Dianpeng Qi[2], Jin Geng[5], Ji Liu[4] & Zhuojun Dai[1]

Plastics are widely used materials that pose an ecological challenge because their wastes are difficult to degrade. Embedding enzymes and biomachinery within polymers could enable the biodegradation and disposal of plastics. However, enzymes rarely function under conditions suitable for polymer processing. Here, we report degradable living plastics by harnessing synthetic biology and polymer engineering. We engineered *Bacillus subtilis* spores harboring the gene circuit for the xylose-inducible secretory expression of *Burkholderia cepacia* lipase (BC-lipase). The spores that were resilient to stresses during material processing were mixed with poly(caprolactone) to produce living plastics in various formats. Spore incorporation did not compromise the physical properties of the materials. Spore recovery was triggered by eroding the plastic surface, after which the BC-lipase released by the germinated cells caused near-complete depolymerization of the polymer matrix. This study showcases a method for fabricating green plastics that can function when the spores are latent and decay when the spores are activated and sheds light on the development of materials for sustainability.

Plastic waste that is improperly disposed of has long been an environmental problem[1,2]. Nature is capable of designing intricate processes and evolving and achieving system-wide, long-term sustainability. In 2016, scientists successfully isolated a bacterium able to degrade and assimilate poly(ethylene terephthalate) (PET) in the soil next to a plastic bottle recycling facility[3,4]. This bacterium produces two enzymes that can hydrolyze PET and the reaction intermediates, shedding light on how to process waste plastics in a sustainable manner. By harnessing the power of these enzymes and material engineering, a different biodegradation route is fabricating special plastics. Efforts have been made to embed enzymes into the polymer matrix to initiate hydrolysis on the surface and bulk, leading to degradation of the matrix[5–8]. However, most enzymes are fragile and sensitive to high temperatures and organic solvents. These conditions are frequently present during plastic processing and can cause enzyme dysfunction and failure during plastic digestion[5,9].

Bacteria have evolved a variety of coping mechanisms to cope with extreme environmental challenges. The most sophisticated, prolonged and textbook example is the formation of spores[10–12]. During reproduction, the cell replicates its genome and divides asymmetrically into two compartments, the endospore and the mother cell. Endospores are coated with multilayered shells that protect the bacterial genome during stressful conditions, including heat, solvents, high pressure

[1]Key Laboratory of Quantitative Synthetic Biology, Shenzhen Institute of Synthetic Biology, Shenzhen Institute of Advanced Technology, Chinese Academy of Sciences, Shenzhen, China. [2]MIIT Key Laboratory of Critical Materials Technology for New Energy Conversion and Storage; National and Local Joint Engineering Laboratory for Synthesis, Transformation and Separation of Extreme Environmental Nutrients, School of Chemistry and Chemical Engineering, Harbin Institute of Technology, Harbin, China. [3]Center of Neural Engineering, CAS Key Laboratory of Human-Machine Intelligence-Synergy Systems, Shenzhen Institute of Advanced Technology, Chinese Academy of Sciences, Shenzhen, China. [4]Department of Mechanical and Energy Engineering, Southern University of Science and Technology, Shenzhen, China. [5]Center for Polymers in Medicine, Shenzhen Institute of Advanced Technology, Chinese Academy of Sciences, Shenzhen, China. [6]These authors contributed equally: Lin Wang, Jing Sun. e-mail: zj.dai@siat.ac.cn

https://doi.org/10.1038/s41589-024-01713-2

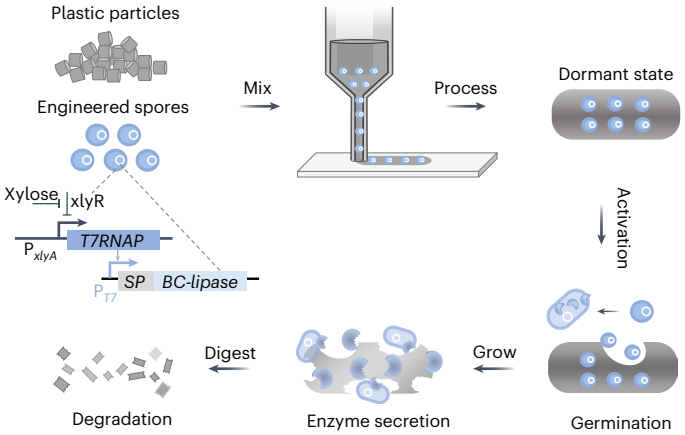

Fig. 1 | Design of the living plastics. The engineered spores and plastic pellets were thoroughly mixed and processed into various formats by 3D printing or solvent casting. The spores were resilient to the material processing conditions. The spore-embedded living plastics performed similarly to ordinary plastics in terms of the material properties when the spores were dormant. The degradation process could be triggered by eroding the surface of the plastics to release the spores. The vegetative cells recovered from the engineered spores secreted specific enzymes and hydrolyzed the polymer, resulting in near-complete degradation of the polymer matrix.

and desiccation[13,14]. Spores can remain dormant indefinitely until the environmental conditions improve, upon which they quickly germinate and resume their vegetative state.

By leveraging synthetic biology and material science, we constructed living plastics by integrating engineered spores inside a polymer-based matrix. We programmed *Bacillus subtilis* with genetic circuits such that the cells can secrete specific enzymes to break down poly(caprolactone) (PCL) and derive spores by induced sporulation. The engineered spores (carrying the circuit), which are invulnerable to high temperatures, organic solvents, high pressure and desiccation, were processed with polymer pellets under stringent material manufacturing conditions to fabricate living plastics in different formats. When the spores are dormant, these spore-embedded living plastics operate like conventional plastics in terms of their physical characteristics and material performance. Then, erosion on the plastic surface activates the dormant spores (Fig. 1). The vegetative cells derived from the spores can then secrete enzymes and hydrolyze the plastic matrix, resulting in near-complete degradation.

Results

Resilience of spores to stresses

We chose *B. subtilis* for this study because it is a model organism that has been extensively investigated and is able to form dormant endospores. We stimulated sporulation by supplementing the nutrients with heavy metal ions (Mn^{2+}). This external stress triggered sporulation and we observed the emergence of both mother cells and spores using microscopy (Fig. 2a). We heated the mixture to 100 °C for 20 min to purify the spores. The staining results indicated that the spores persisted while the free cells were mostly eliminated (Fig. 2b and Supplementary Fig. 1). To verify that the spores were resistant to both high temperatures and organic solvents, we heated the obtained spores at temperatures ranging from 85 to 120 °C and inoculated the treated spores in Luria–Bertani (LB) medium. All spores rapidly recovered from heat shock (Fig. 2b,c) and reached a similar cell density after 24 h (Fig. 2d). However, no growth was observed for *B. subtilis* cells following the same treatment (85–120 °C for 20 min), confirming the sensitivity of the vegetative cells (Supplementary Fig. 2).

We also tracked spore recovery in nutrients (LB medium) after exposure to a toluene-based organic solvent for a range of durations. Even after being soaked in toluene for 24 h, the spores recovered from the stress and subsequently grew to an optical density (OD) similar to that of the untreated spores (Fig. 2e). These collective results confirmed the capacity of the spores to adapt to harsh conditions, which could shield the cells from the extreme stresses associated with plastic processing.

Engineering spores to secrete PCL-degrading enzymes

To engineer spores harboring the genetic information for a particular protein expression and secretion, we transformed the gene circuit into *B. subtilis* and induced sporulation. Briefly, *B. subtilis* host cells were engineered to incorporate a DNA cassette that expresses T7 RNA polymerase under the control of a D-xylose-inducible promoter (P_{xylA})[15]. The cells were subsequently transformed with a genetic circuit containing a T7 promoter and the target gene. The addition of xylose induced the expression of T7 RNA polymerase, which bound to the T7 promoter and drove the expression of the downstream gene of interest. We used a T7-controlled green fluorescent protein (GFP) expression plasmid as the model system to investigate whether the germinated cells originating from the spores could maintain the designed features (Supplementary Tables 1 and 2). The results revealed that the cells recovered from the circuit-engineered spores exhibited remarkable GFP fluorescence (~31.7 times higher intensity; Supplementary Table 3). Nevertheless, this signal was not observed in the germinated spores without the plasmid (Fig. 3a). The impact of extrinsic stressors, such as high temperature or solvent dissolution, on the passage, maintenance and expression of genetic information was subsequently quantified. We collected the engineered spores and stressed them with heat (120 °C for 20 min) or organic solvent (soaking in toluene for 48 h). The processed spores were then recovered in LB medium and the vegetative cells were collected and subjected to flow cytometric analysis. We counted the glowing cells among the sorted cells (10,000 cells in total). The quantitative data confirmed that the cells recovered from the treated and untreated spores and the normal cells harboring the GFP plasmid all had similar percentages of fluorescent individuals (Fig. 3b,c and Supplementary Fig. 3). These combined findings suggested that engineered spore-derived cells could sustain the desired capabilities despite exposure to challenging environmental conditions.

We then engineered spores that could secrete *Burkholderia cepacia* lipase (BC-lipase) after resuming the vegetative cell cycle. The ability of BC-lipase to hydrolyze PCL because of its distinctive structure has been well investigated[16–18]. The deep and narrow hydrophobic cleft from the surface of BC-lipase to the catalytic triad facilitates substrate polymer chain sliding while preventing dissociation (Fig. 3d). Six polar residues are also located in front of the hydrophobic binding region, driving the polymer chain forward following hydrolysis. To regulate enzyme expression, the BC-lipase gene, which has a secretory tag at the N terminus for enzyme export, was positioned downstream of the T7 promoter (Fig. 3e and Supplementary Tables 1 and 2). Cells transformed with the circuit were cultured in the presence of nutrients (LB medium) and the supernatant was collected and purified for SDS–PAGE and matrix-assisted laser desorption ionization–time-of-flight (MALDI–TOF) analysis. The results confirmed the presence of the desired protein, indicating that the engineered cells successfully produced and delivered the enzyme to the extracellular environment (Fig. 3e,f). Quantitative analysis revealed that ~67% of the expressed BC-lipase was secreted into the supernatant, for a yield of ~9.17 mg l^{-1} (~167 U per liter activity) (Supplementary Fig. 4a–c). Induction with xylose had a minimal effect on cell growth (Supplementary Fig. 4d).

To assess the function of the secreted BC-lipase, we incubated the *B. subtilis* culture with standard PCL films. Inducing BC-lipase expression caused erosion of the PCL films (Fig. 3g). This breakdown was also observed on the remaining pieces after multisite digestion by scanning electron microscopy (SEM) (Fig. 3h and Supplementary Fig. 5). The digestion process and shift in the molar mass of the digested

https://doi.org/10.1038/s41589-024-01713-2

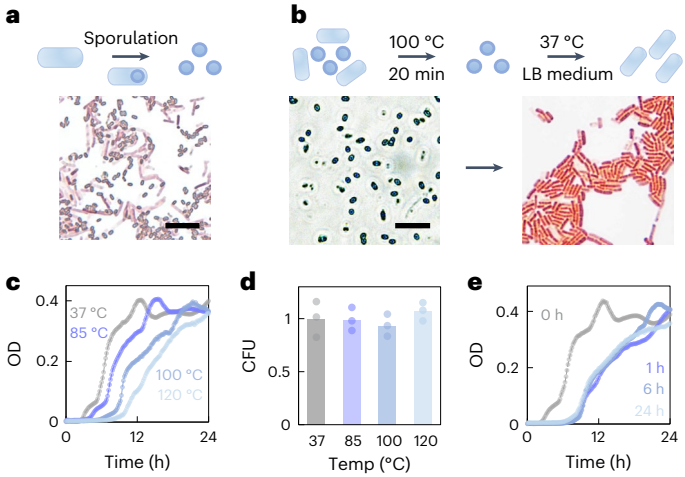

Fig. 2 | The spores were resilient to environmental perturbations. a, Induced sporulation of *B. subtilis*. Top, schematic; bottom, experimental data. Spores and vegetative cells were stained with malachite green and safranine solution, respectively. Scale bar, 10 µm. **b**, Spores heated at high temperatures resumed vegetative growth after supplementing their nutrition. Top, schematic; bottom, experimental data. The spores were purified by heating the mixture to 100 °C for 20 min to eliminate most of the vegetative cells. After being inoculated into LB medium, the purified spores (left) returned to their life cycle (right), as observed by fluorescence microscopy. Scale bar, 10 µm. **c**, Growth curve reflecting the resilience of the spores to heat shock at various temperatures. Spores heated to different temperatures for 20 min were resuspended and cultivated in LB medium at 37 °C. **d**, After exposure to nutrients, the spores that were heated at various temperatures reached a comparable cell density. Cell density was measured by CFU counting after the culturing of treated spores in LB medium for 24 h. The data were normalized by the CFU value of the culture grown from spores without heating (37 °C). The columns indicate the mean values ($n = 3$). **e**, Growth curve reflecting the resilience of the spores to toluene. Toluene-soaked spores were resuspended in LB medium and cultivated at 37 °C. The numbers indicate the treatment durations. The experiments in **a**–**e** were repeated independently more than three times with similar results.

product were traced by gel permeation chromatography (GPC), and the results revealed a substantial loss of weight in the PCL matrix (there was a smaller primary peak area after digestion than that of the PCL films without incubation in induced cell culture) and the emergence of degradation byproducts (peaks with longer retention times), which are indicative of effective enzyme processing (Fig. 3i and Supplementary Fig. 6). These engineered *B. subtilis* cells were then induced to sporulate, after which the spores were collected and purified for subsequent material processing.

Fabrication of spore-embedded living PCL films

By exploiting the engineered spores, we continued to develop degradable living materials with different formats by embedding the spores inside a solvent-dissolved or melted PCL matrix. We used a conventional solvent-casting technique to prepare spore-embedded PCL plastic films (living films). PCL pellets were dissolved in toluene and then mixed with the engineered spores until the spores were homogeneously distributed. The mixture was cast onto a 6-inch monocrystalline silicon wafer and the films precipitated after solvent evaporation. The regular and spore-embedded PCL films did not appear to be notably different (Fig. 4a). Additional microscopic investigations revealed that the spore clusters were dispersed throughout the living films (Fig. 4b). To compare the physical characteristics of the materials, we measured the tensile strength and melting temperature (by differential scanning calorimetry (DSC)) of both the living and the regular PCL films. As shown in Fig. 4c,d and Supplementary Figs. 7 and 8, there were no discernible differences between the two groups, indicating that the living films could be used for regular service conditions when the spores were dormant.

The degradation of living films could be triggered. We selected *Candida antarctica* lipase (CA-lipase) as the triggering agent because it has a surface-exposed, shallow active site that can erode the plastic surface through a random scission pathway to release the spores (Fig. 4e and Supplementary Fig. 9)[19,20]. The living PCL films remained stable while the spores were dormant (images were taken on day 7; Fig. 4f). Adding CA-lipase caused only partial degradation of the regular PCL films (Fig. 4g, left), similar to the results reported by other studies[7,8]. In contrast, CA-lipase addition triggered the release and germination of the spores from the living films. These vegetative cells secreted BC-lipase after induction and thoroughly degraded the remaining films (images were taken on day 7; Fig. 4g, right). The viability of the living cells was determined by quantitative analysis. Both the weight and the molar mass data (obtained by GPC) indicated that the induction of germination (with the addition of xylose and CA-lipase) caused BC-lipase to be expressed and nearly completely degrade the films (Fig. 4h,i and Supplementary Fig. 10a) while, in the absence of induction (with the addition of CA-lipase), only partial film assimilation was observed (Fig. 4h and Supplementary Fig. 10b). Efficient degradation of the living films was feasible in compost tests when CA-lipase was not present, as determined by a standard testing agency (Supplementary Fig. 11). We also conducted an in-house test using industrial soil composts (Fig. 4j and Supplementary Figs. 12–15). Without CA-lipase supplementation, the living films showed accelerated depolymerization and disintegrated within 30 days within the operating temperature range of industrial compost facilities (Supplementary Fig. 14, with xylose). In contrast, the regular films required an additional 20–25 days to decompose into sample fragments that were no longer visible, possibly because of the existence of various microbes in the compost soil (Supplementary Fig. 15).

Fabrication of spore-embedded living PCL plastic objects

Lastly, using a high-temperature nozzle, we extruded the mixture of melted PCL pellets and purified spores to create three-dimensional (3D) PCL plastic objects (Fig. 5a and Supplementary Fig. 16). To ensure the melting and printability of the pellets, the blend was held in a heated nozzle (120 °C) for 10 min. This stress could be detrimental to the pure enzyme[21]. The regular PCL material incubated with heated BC-lipase (5 mg ml^{-1}) showed no evidence of polymer digestion after 30 days, suggesting that high-temperature processing caused the enzyme to become dysfunctional (Fig. 5b and Supplementary Fig. 17). In contrast, the spores were able to withstand this stress. After coculturing the plastic films with the germinated cells from the heated spores, the matrix eroded, confirming the activity of the enzyme (Fig. 5c).

The living PCL plastics (generated by fused filament fabrication) remained stable while the spores were dormant (Fig. 5d). Then, CA-lipase dissolved the plastic stick surface and activated the spores. The cells were revived under induction, causing the ultimate destruction of the 3D-printed living plastics, while the noninduced living plastics (supplemented with CA-lipase) or regular 3D-printed plastics treated with CA-lipase were only partially assimilated (Fig. 5e,f and Supplementary Fig. 18). The GPC results revealed the gradual breakdown of the PCL matrix and a shift in the molar mass, as indicated by the weight loss from the living PCL sticks (primary peak) and the emergence of degradation byproducts (peaks with longer retention times) (Supplementary Fig. 18c,d). In line with the data shown in Fig. 5e,f, both peaks vanished entirely within 6–7 days, indicating the near-complete disintegration of the 3D-printed plastics (Fig. 5g). Without induction, the weight-average molar mass (M_w) of the 3D-printed living object decreased to ~31,000 g mol^{-1} (~65% of the original M_w) after 7 days and was still greater than 21,000 g mol^{-1} after 20 days when treated with CA-lipase only (Supplementary Fig. 18d). The byproducts (6 days from living plastics) were further examined by liquid chromatography–mass

https://doi.org/10.1038/s41589-024-01713-2

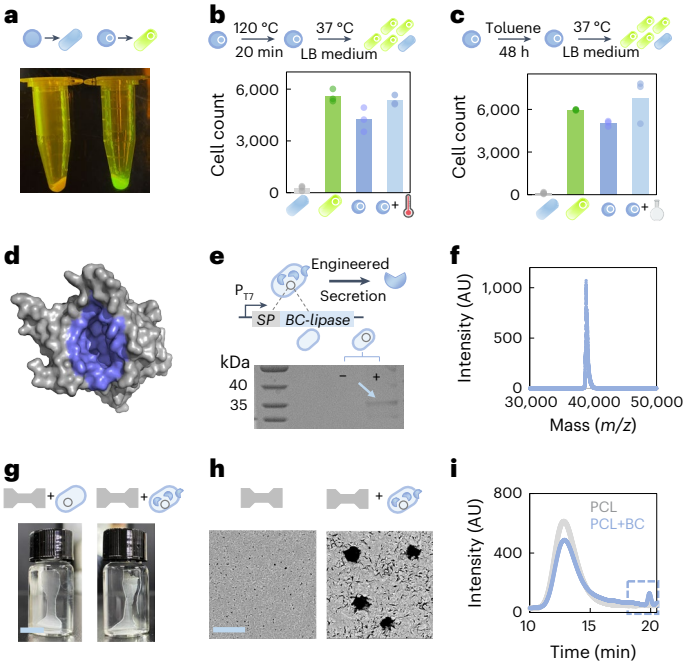

Fig. 3 | Spores were engineered to secrete PCL-degrading enzymes. a, Circuit-engineered spores expressed the desired protein after germination. The GFP signal was observed only in cells retrieved from spores carrying the genetic circuit. **b**, High temperatures did not impede the storage or passage of genetic information. Cells that did or did not harbor the GFP circuit and germinated cells from untreated or treated (heated to 120 °C for 20 min) spores (both bearing the GFP circuit) were analyzed by flow cytometry (10,000 cells were counted). The number of fluorescent cells was quantified for each sample. The columns indicate the mean values ($n = 3$). **c**, Treatment with an organic solvent had no adverse effect on the storage or transmission of genetic information. The quantitative approach was the same as that in **b**. The columns indicate the mean values ($n = 3$). **d**, Effective PCL digestion was facilitated by the distinctive structure of BC-lipase. Surface illustration of BC-lipase (Protein Data Bank 3LIP) highlighting the substrate binding pocket (colored slate). **e**, Engineering *B. subtilis* to secrete BC-lipase. The BC-lipase gene was fused with a secretion peptide (SP). The secretory expression of the desired protein was verified by SDS–PAGE. **f**, The MALDI–TOF results confirmed the expression of BC-lipase. The *m/z* value of the detected peak complied with the apparent molecular mass of BC-lipase (38.4 kDa). AU, arbitrary units. **g**, PCL films were partially decomposed in the induced culture of engineered *B. subtilis*. PCL films were immersed in the engineered *B. subtilis* culture with (right) or without (left) induction. After induction, clear partial digestion of the films was induced by secretory BC-lipase expression on day 12. Scale bar, 0.75 cm. **h**, SEM revealed that after induction, the cultured engineered *B. subtilis* eroded the films (12 days). Scale bar, 80 µm. **i**, GPC results validated the decomposition of PCL. Coculturing PCL films with engineered *B. subtilis* caused shrinkage of the PCL primary peak and the emergence of a side product peak (day 12). The experiments in **a**–**c** and **e**–**i** were repeated independently more than three times with similar results.

spectrometry (LC–MS) and the results showed that the main components were small molecules less than 500 Da that may be associated with the metabolic pathway of the bacterium (Fig. 5h and Supplementary Figs. 19 and 20).

Discussion

The invention of plastics has transformed daily life by replacing natural materials with synthetic counterparts that are typically lighter, more stable, mechanically robust and cost effective. However, the rapid increase in the creation of disposable plastic products has outpaced nature's capacity to dispose of them, making plastic pollution one of the most pressing environmental challenges. Several investigations have recently discovered novel enzymes that can break down plastics. These efforts have thus far concentrated on identifying, designing and evolving enzymes with improved catalytic activity toward plastic degradation[22,23]. An alternative strategy to combat this problem is to engineer special plastics; thus, embedding pure enzymes inside a polymer matrix has been investigated. However, implementation of this method remains challenging because of the incompatibility between the stringent processing conditions of plastic products and enzyme sensitivity (for example, Fig. 5b)[6,24–26]. By exploiting the innate strategies of microorganisms for surviving extreme environmental challenges and engineering tools from synthetic biology (Figs. 2 and 5c), we developed spore-embedded plastics to offer new insights into the fabrication of environmentally friendly materials. Our technology is modular by design; the target enzymes, the bacterial strain and the polymer matrix may each be tuned separately before being combined. The same design approach can be applied to various alternative polymers, enzymes, triggers to release the spores and production techniques

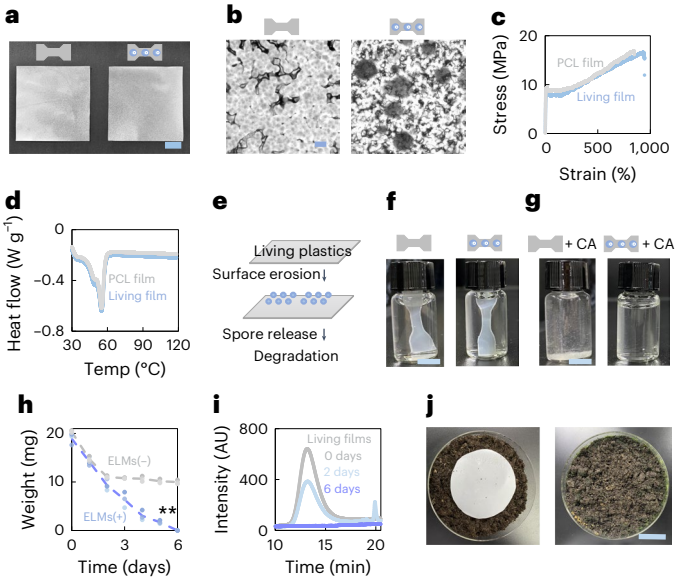

Fig. 4 | Fabrication of living PCL films. a, Fabrication of spore-embedded PCL films. Scale bar, 1 cm. **b**, Spores were distributed throughout the living films. Right, microscopy images demonstrating the scattered distribution of clustered spores inside the living films. Scale bar, 100 µm. **c**, Tensile test data reflecting the negligible change in the mechanical properties between the regular and living films. **d**, DSC measurements revealing the similar melting temperatures for the regular and living films. **e**, Schematic showing that external cues triggered the release of spores from the living films. CA-lipase eroded the surface of the living films to release spores. The recovered cells secreted BC-lipase and digested the remaining films. **f**, The integrity of the living films was maintained without external cues. Scale bar, 0.75 cm. **g**, The living films were nearly thoroughly digested upon exposure to an external stimulus. Adding CA-lipase to the living films caused the release of the spores and their reversion to vegetative cells. Upon induction, the living films were nearly completely degraded because of the expression of BC-lipase. In comparison, adding CA-lipase to the regular films caused only partial degradation of the material. The images in **f** and **g** were taken on day 7. Scale bar, 0.75 cm. **h**, Quantitative analysis of the digestion process. After induction, the living films were nearly completely decomposed within 6 days. CA-lipase was added to both samples. The dashed lines indicate the means ($n = 3$). $^{**}P < 0.01$ ($P = 0.0005$ on day 6) for engineered living materials (ELMs) with (+) and without (−) induction, as determined by a two-sided Student's two-sample *t*-test assuming unequal variances. **i**, GPC results confirmed the near-complete degradation of the living films (ELMs+). On day 6, both the main peak and the side product peak vanished. **j**, The living films showed accelerated depolymerization in industrial soil composts. The images show the degradation of living films on day 0 (left) and day 36 (right). CA-lipase was not added. Scale bar, 5 cm. The experiments in **a**–**d** and **f**–**j** were repeated independently more than three times with similar results.

https://doi.org/10.1038/s41589-024-01713-2

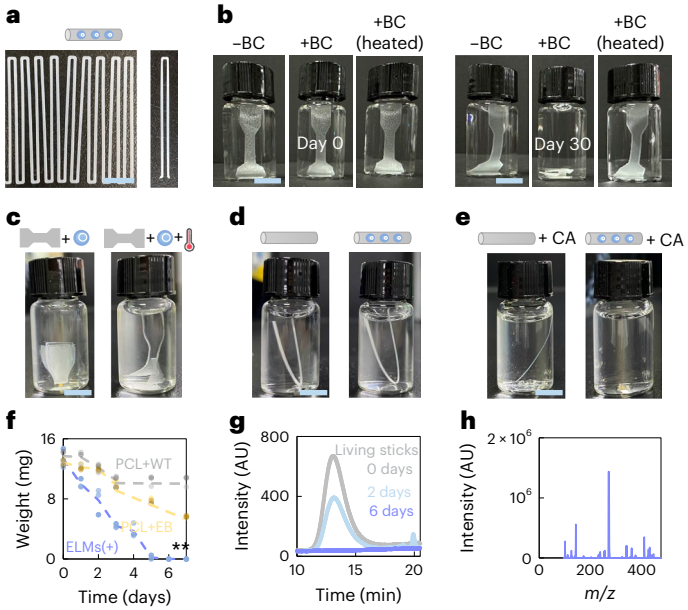

Fig. 5 | Fabrication of living PCL objects by fused filament fabrication. **a**, Living plastics containing engineered spores were fabricated by a 3D printer. Scale bar, 1 cm. **b**, Heated BC-lipase lost its ability to digest PCL films. Regular PCL films incubated with heated BC-lipase showed no evidence of polymer digestion after 30 days, indicating that high-temperature processing (120 °C, 10 min) led to enzyme dysfunction. Scale bar, 0.75 cm (**b**–**e**). **c**, The spores retained their engineered functions regardless of the heat treatment. Digestion of regular PCL films was observed by germinated spores without (left) or with (right) heat treatment (120 °C, 10 min). Images were taken on day 22. **d**, The integrity of the 3D-printed living plastics was maintained without external triggers. The images show regular (left) and living (right) plastics. **e**, The 3D-printed living plastics were nearly completely digested because of the germination of the engineered spores. The addition of CA-lipase promoted the release of the spores and their conversion to vegetative cells. Upon induction, the living plastics were nearly completely degraded because of the expression of BC-lipase. Comparatively, the regular sticks were only partially degraded when CA-lipase was added. All the images in **d** and **e** were taken on day 7. **f**, Quantitative analysis of plastic breakdown. The samples included 3D-printed living plastics induced by xylose (ELMs+) and regular 3D-printed PCL plastics cocultured with wild-type cells not carrying the genetic circuit (PCL + WT) or engineered *B. subtilis* (cells carrying the genetic circuit, PCL + EB). The dashed lines indicate the means ($n = 3$). $^{**}P < 0.01$ ($P = 0.00024$ and 0.0016 on day 7 for ELMs+ compared to PCL + EB and PCL + WT, respectively, as determined by a two-sided Student's two-sample t-test assuming unequal variances). **g**, The 3D-printed living plastics nearly completely disintegrated. Both the primary peak and the side product peak vanished within 6 days. **h**, LC–MS verification that the degradation byproducts of the living plastics were small molecules. The majority of the byproducts had a mass of less than 500 Da. The experiments in **a**–**h** were repeated independently more than three times with similar results.

(for example, single-screw extruder). To this end, we created a variety of living plastics by integrating engineered spores (which carry the GFP expression circuit) with different polymer systems (including PET) at processing temperatures ranging from 150 to 300 °C (Supplementary Fig. 21). In the present study, we used CA-lipase to release the spores because enzymatic treatment is mild and can be standardized for reproducibility and subsequent use. Alternative approaches to liberate spores could be applied. To demonstrate this possibility, we ground the generated living plastics and verified that the spores could endure the stress of grinding and be released from the matrix, as indicated by the presence of glowing bacteria after culture (Supplementary Fig. 22). Moreover, we placed the living films in boiling medium to release the spores and the activated spores germinated and performed the desired function (Supplementary Fig. 23). We also processed the living PCL with a single-screw extruder. The living material degradation profile was similar to that of the living PCL films and 3D-printed objects (Supplementary Fig. 24). The living plastics remained stable when soaked in soda (Sprite) for 60 days, suggesting their potential use as packaging materials (Supplementary Fig. 25). Because of their resilience to desiccation, spore-containing materials can be stored indefinitely until favorable growth conditions are sensed.

B. subtilis is found in a wide variety of environments and *Bacillus* species are mostly considered soil dwelling[27]. *Bacillus* species are not pathogenic and are particularly intriguing as potential probiotics[28]. Furthermore, *B. subtilis* can adapt to grow at elevated temperatures even above 60 °C (refs. 29–32), making them a potent candidate strain used during industrial compost conditions (Supplementary Fig. 26). Collectively, these traits make *B. subtilis* a strong candidate for use in the field. In contrast to pure enzymes, which are susceptible to environmental changes, living cells can consistently produce and secrete target enzymes to efficiently degrade plastics[33–35]. Evaluation of plasmid persistence indicated that ~5×10^4 cells (starting from ~10^8) maintained their engineered function (including maintenance of the chloramphenicol resistance and gene of BC-lipase) after 20 days without selection pressure (Supplementary Fig. 27). The living plastics were able to thoroughly disintegrate without the addition of antibiotics, underscoring the robustness of the system (Supplementary Figs. 14 and 28). Our study offers new perspectives on creating living materials. The method presented here might benefit areas including sustainable materials, biofabrication and bioenergy.

Online content

Any methods, additional references, Nature Portfolio reporting summaries, source data, extended data, supplementary information, acknowledgements, peer review information; details of author contributions and competing interests; and statements of data and code availability are available at https://doi.org/10.1038/s41589-024-01713-2.

References

1. Law, K. L. & Narayan, R. Reducing environmental plastic pollution by designing polymer materials for managed end-of-life. *Nat. Rev. Mater.* **7**, 104–116 (2022).
2. Stubbins, A., Law, K. L., Munoz, S. E., Bianchi, T. S. & Zhu, L. X. Plastics in the Earth system. *Science* **373**, 51–55 (2021).
3. Yoshida, S. et al. A bacterium that degrades and assimilates poly(ethylene terephthalate). *Science* **351**, 1196–1199 (2016).
4. Tournier, V. et al. An engineered PET depolymerase to break down and recycle plastic bottles. *Nature* **580**, 216–219 (2020).
5. Huang, Q., Hiyama, M., Kabe, T., Kimura, S. & Iwata, T. Enzymatic self-biodegradation of poly(L-lactic acid) films by embedded heat-treated and immobilized proteinase K. *Biomacromolecules* **21**, 3301–3307 (2020).
6. Khan, I., Nagarjuna, R., Dutta, J. R. & Ganesan, R. Enzyme-embedded degradation of poly(ε-caprolactone) using lipase-derived from probiotic *Lactobacillus plantarum*. *ACS Omega* **4**, 2844–2852 (2019).
7. DelRe, C. et al. Near-complete depolymerization of polyesters with nano-dispersed enzymes. *Nature* **592**, 558–563 (2021).
8. DelRe, C. et al. Synergistic enzyme mixtures to realize near-complete depolymerization in biodegradable polymer/additive blends. *Adv. Mater.* **33**, e2105707 (2021).
9. Panganiban, B. et al. Random heteropolymers preserve protein function in foreign environments. *Science* **359**, 1239–1243 (2018).
10. Tan, I. S. & Ramamurthi, K. S. Spore formation in *Bacillus subtilis*. *Environ. Microbiol. Rep.* **6**, 212–225 (2014).
11. Higgins, D. & Dworkin, J. Recent progress in *Bacillus subtilis* sporulation. *FEMS Microbiol. Rev.* **36**, 131–148 (2012).
12. McKenney, P. T., Driks, A. & Eichenberger, P. The *Bacillus subtilis* endospore: assembly and functions of the multilayered coat. *Nat. Rev. Microbiol.* **11**, 33–44 (2013).

13. González, L. M., Mukhitov, N. & Voigt, C. A. Resilient living materials built by printing bacterial spores. *Nat. Chem. Biol.* **16**, 126–133 (2020).
14. Yang, M. et al. Engineering *Bacillus subtilis* as a versatile and stable platform for production of nanobodies. *Appl. Environ. Microbiol.* **86**, e02938-19 (2020).
15. Ji, M. et al. A wheat bran inducible expression system for the efficient production of α-L-arabinofuranosidase in *Bacillus subtilis*. *Enzym. Microb. Technol.* **144**, 109726 (2021).
16. Sanchez, D. A., Tonetto, G. M. & Ferreira, M. L. *Burkholderia cepacia* lipase: a versatile catalyst in synthesis reactions. *Biotechnol. Bioeng.* **115**, 6–24 (2018).
17. Horn, S. J. et al. Costs and benefits of processivity in enzymatic degradation of recalcitrant polysaccharides. *Proc. Natl Acad. Sci. USA* **103**, 18089–18094 (2006).
18. Breyer, W. A. & Matthews, B. W. Structure of *Escherichia coli* exonuclease I suggests how processivity is achieved. *Nat. Struct. Biol.* **7**, 1125–1128 (2000).
19. Ericsson, D. J. et al. X-ray structure of *Candida antarctica* lipase A shows a novel lid structure and a likely mode of interfacial activation. *J. Mol. Biol.* **376**, 109–119 (2008).
20. Widmann, M., Juhl, P. B. & Pleiss, J. Structural classification by the Lipase Engineering Database: a case study of *Candida antarctica* lipase A. *BMC Genom.* **11**, 123 (2010).
21. Sugihara, A., Ueshima, M., Shimada, Y., Tsunasawa, S. & Tominaga, Y. Purification and characterization of a novel thermostable lipase from *Pseudomonas cepacia*. *J. Biochem.* **112**, 598–603 (1992).
22. Lu, H. et al. Machine learning-aided engineering of hydrolases for PET depolymerization. *Nature* **604**, 662–667 (2022).
23. Sanluis-Verdes, A. et al. Wax worm saliva and the enzymes therein are the key to polyethylene degradation by *Galleria mellonella*. *Nat. Commun.* **13**, 5568 (2022).
24. Stepankova, V. et al. Strategies for stabilization of enzymes in organic solvents. *ACS Catal.* **3**, 2823–2836 (2013).
25. Daniel, R. M. & Danson, M. J. Temperature and the catalytic activity of enzymes: a fresh understanding. *FEBS Lett.* **587**, 2738–2743 (2013).
26. Ganesh, M., Dave, R. N., L'Amoreaux, W. & Gross, R. A. Embedded enzymatic biomaterial degradation. *Macromolecules* **42**, 6836–6839 (2009).
27. Beauregard, P. B., Chai, Y., Vlamakis, H., Losick, R. & Kolter, R. *Bacillus subtilis* biofilm induction by plant polysaccharides. *Proc. Natl Acad. Sci. USA* **110**, E1621–E1630 (2013).
28. Su, Y., Liu, C., Fang, H. & Zhang, D. W. *Bacillus subtilis*: a universal cell factory for industry, agriculture, biomaterials and medicine. *Microb. Cell Fact.* **19**, 173 (2020).
29. Dubay, M. M. et al. Quantification of motility in *Bacillus subtilis* at temperatures up to 84 °C using a submersible volumetric microscope and automated tracking. *Front. Microbiol.* **13**, 836808 (2022).
30. Warth, A. D. Relationship between the heat resistance of spores and the optimum and maximum growth temperatures of *Bacillus* species. *J. Bacteriol.* **134**, 699–705 (1978).
31. Hecker, M., Schumann, W. & Volker, U. Heat-shock and general stress response in *Bacillus subtilis*. *Mol. Microbiol.* **19**, 417–428 (1996).
32. Msadek, T., Kunst, F. & Rapoport, G. MecB of *Bacillus subtilis*, a member of the ClpC ATPase family, is a pleiotropic regulator controlling competence gene expression and growth at high temperature. *Proc. Natl Acad. Sci. USA* **91**, 5788–5792 (1994).
33. Nguyen, P. Q., Courchesne, N. M. D., Duraj-Thatte, A., Praveschotinunt, P. & Joshi, N. S. Engineered living materials: prospects and challenges for using biological systems to direct the assembly of smart materials. *Adv. Mater.* **30**, e1704847 (2018).
34. Molinari, S., Tesoriero, R. F. & Ajo-Franklin, C. M. Bottom-up approaches to engineered living materials: challenges and future directions. *Matter* **4**, 3095–3120 (2021).
35. Zhu, R. et al. Engineering functional materials through bacteria-assisted living grafting. *Cell Syst.* **15**, 264–274 (2024).

Methods

Strains, circuits and media

Bacterial strains. *B. subtilis* 164s-T7, which incorporated a D-xylose-inducible T7 RNA polymerase on the genome, was used to generate spores[15]. Plasmids carrying the gene of interest under the control of a T7 promoter were then introduced into *B. subtilis* for sporulation.

Circuits and plasmids. The fragment of BC-lipase was synthesized and assembled in a pMK4 vector between XbaI and EcoRI by Tsingke Biotechnology. Details of the sequence can be found in Supplementary Tables 1 and 2.

Growth media. *LB medium*. First, 25 g of LB broth powder (Aladdin, Shanghai, China) was added into 1 L of deionized H_2O. After autoclaving for 45 min, the LB medium was stored at room temperature.

All medium used was supplemented with appropriate antibiotics (10 μg ml^{-1} chloramphenicol) when applicable. Furthermore, 5 mg ml^{-1} xylose was used to induce gene expression when applicable. Agar (2% Bacto, BD) was dissolved in the liquid medium to prepare the related agar plate.

Materials. *PCL and other plastics*. PCL pellets (type no. 6800), poly(butylene adipate-*co*-terephthalate) (PBAT), poly(butylene succinate) (PBS), poly(lactic acid) (PLA), polyhydroxyalkanoates (PHAs) and PET were purchased from Haise Plastic.

Methods

Overnight liquid culture. *B. subtilis* was streaked onto a plate of LB agar and incubated at 37 °C for 16 h. Then, a single colony was picked and inoculated in 3 ml of LB medium. The bacterial culture was placed in a shaking incubator (temperature, 37 °C; shaking speed, 220 r.p.m.). The agar plate and liquid medium were supplemented with appropriate antibiotics when applicable.

Sporulation induction. Overnight cultures of *B. subtilis* were prepared as described above, streaked onto a plate of LB agar supplemented with 50 mg l^{-1} Mn^{2+} and incubated at 37 °C for 7 days. The spores were collected by washing off the plate surface using autoclaved deionized water and centrifuging at 4 °C (4,602*g*) for 15 min. The washing and centrifugation procedures were repeated five times and the collected spores were stored at 4 °C in deionized water. The spore solution was heated in a metal bath at 100 °C for 20 min and cooled to room temperature before use to eliminate the vegetative cells.

Spore germination. The solution of purified spores (OD_{600} ≈ 18) was inoculated into LB medium with appropriate antibiotics (10 μg ml^{-1} chloramphenicol). The inoculated culture was placed in a shaker at 37 °C and 220 r.p.m. to prepare overnight culture.

Staining method for spores and vegetative cells. The spores and *B. subtilis* cells were washed off by deionized water from the sporulation agar plate. Then, 20 μl of the mixture was added onto a glass slide and spread evenly. The slides were heated by an alcohol burner for 30 s to immobilize the spores and *B. subtilis*. To stain the spores, 100 μl of malachite green staining solution (Hopebio) was added onto the slide and the slide was again heated by an alcohol burner for 30 s. After cooling down, the remaining staining solution was washed off by deionized water. To stain the vegetative cells, 100 μl of safranine staining solution (Hopebio) was added onto the slide and incubated for 60 s. The remaining staining solution was washed off by deionized water. Fluorescence microscopy (Nikon Ti2-E) was used to check whether spores or *B. subtilis* cells were successfully stained by specific solutions. NIS-Elements software (version 11.0.0.28844) was used for collecting microscopic images.

Growth curve measurement. The purified spores (OD_{600} ≈ 18) were heated by a metal bath at 85 °C, 100 °C and 120 °C or soaked in toluene for 1 h, 6 h and 24 h (replacing the water with the same volume of toluene). Then, 2 μl of heated or solvent-treated spores were inoculated into 200 μl of LB medium supplemented with 10 μg ml^{-1} chloramphenicol. The wells were then sealed with 50 μl of mineral oil to prevent evaporation. We measured the OD_{600} of cultures with a plate reader (Tecan, Infinite 200 PRO). Then, i-control 2.0 software was used for collecting absorbance and fluorescence data with the plate reader (TECAN).

To evaluate the effect of xylose on the growth of *B. subtilis*, we monitored the growth of cells in medium with or without xylose. A single colony of *B. subtilis* (carrying the T7 construct) was inoculated in 3 ml of LB medium containing antibiotics and cultured overnight at 37 °C (shaking speed, 220 r.p.m.). Then, we diluted the calibrated cultures (1:100) into LB medium with antibiotics. The diluted cultures (200 μl) were aliquoted into 96-well plates and then sealed with 50 μl of mineral oil to prevent evaporation. We measured the optical density of cultures (OD_{600}) using a plate reader (BioTek Synergy H1). Gen5 CHS software (version 3.08) was used for collecting absorbance and fluorescence data from the plate reader (Biotek). For data analysis, the measured OD_{600} values were background corrected.

Evaluation of the intensity of fluorescent protein. Germinated *B. subtilis* cells carrying or not carrying the GFP expression circuit were pregrown in LB medium with the appropriate antibiotics overnight. Then, 20 μl of overnight culture was inoculated into 3 ml of LB medium at 37 °C for 24 h. Next, 5 mg ml^{-1} xylose (final concentration) was used to induce the protein expression. The culture was diluted tenfold using sterilized water. A 200-μl sample was then analyzed by a plate reader (BioTek Synergy H1), with the excitation at 480 nm and the emission at 520 nm. The measured value was corrected by subtracting the blank and then divided by the corresponding OD to obtain the data.

Protein expression and examination. *B. subtilis* cells carrying the protein expression circuit were pregrown in LB medium with the appropriate antibiotics overnight. Then, 1 ml of overnight culture was inoculated into 100 ml of LB medium at 37 °C. Next, 5 mg ml^{-1} xylose was used to induce the protein expression and secretion. The supernatant of the culture was collected, purified and analyzed. For His-tag affinity purification, 100 μl of cOmplete His-tag purification resin (Sigma-Aldrich) was used to bind 100 ml of supernatant. The resin was washed with washing buffer and eluted with 50 μl of elution buffer (20 mM Tris, 500 mM NaCl, 250 mM imidazole and 5% glycerol). The protein was verified by SDS–PAGE with Coomassie blue staining.

Flow cytometry. The cell culture was diluted 800-fold using 1× phosphate-buffered saline (Solarbio, P1010). The sample was then analyzed by flow cytometry (Beckman Coulter CytoFLEX S). Fluorescence was measured for >10,000 events for each sample. We used the CytExpert software (version 2.5.0.77) for data collection. The FITC channel was chosen for GFP measurement. Data were processed using FlowJo (version 10.6.2) to obtain the median of fluorescence, autogated by the height of the forward scatter and the side scatter (FSC-H/SSC-H). FITC-H ≥ 9.0 kV was identified as a cell with a green fluorescent signal.

Evaluation of lipase activity and secretion yield. *B. subtilis* cells carrying the protein expression circuit were pregrown in LB medium with the appropriate antibiotics overnight. Then, 20 μl of overnight culture was inoculated into 3 ml of LB medium at 37 °C for 24 h. Next, 5 mg ml^{-1} xylose was used to induce the protein expression and secretion. The supernatant of the culture was collected and analyzed. We used *p*-nitrophenyl palmitate (p-NPP) as the reaction substrate and the hydrolytic activity of the BC-lipase was associated with the generation of *p*-nitrophenol (p-NP), reflected by the increase in absorbance at 405 nm. We generated the calibration curve by plotting the known

concentration of p-NP (Sigma-Aldrich, 241326) against its absorbance at 405 nm. The concentration of synthesized p-NP by the hydrolytic reaction was then determined by the calibration curve. We then calculated the consumed p-NPP on the basis of the generated p-NP. The reaction system comprised 450 µl of Tris-HCl buffer (50 mM, pH 8.5), 20 µl of anhydrous ethanol, 5 µl of p-NPP (10 mM, dissolved in acetonitrile) and 25 µl of supernatant. The reaction system was shaken, mixed and then placed in a water bath of 45 °C for 20 min. At the end of the reaction, 200 µl of the reaction system was transferred to a 96-well plate for absorbance measurement (405 nm, Tecan, Infinite E PLEX). Here, 1 U was defined as the amount of enzyme that catalyzes the conversion of 1 µmol of substrate per min.

To quantify the yield of BC-lipase, we prepared a series of lipase solutions (Sigma-Aldrich, 534641) in different concentrations and reacted with the substrate. The reaction system comprised 450 µl of Tris-HCl buffer (50 mM, pH 8.5), 20 µl of anhydrous ethanol, 5 µl of p-NPP (10 mM, dissolved in acetonitrile) and 25 µl of calibration samples in different concentrations. We generated the calibration curve by plotting the known lipase concentration against the reaction absorbance at 405 nm (correlated with the generated p-NP). The BC-lipase in the supernatant was then calculated using the calibration curve.

MALDI–TOF analysis. First, 1 µl of purified BC-lipase solution was smeared onto MTP 384 polished steel targets (Bruker Daltonics). Then, 1 µl of sinapinic acid (SA) solution (20 mg ml^{-1}, acetonitrile:H_2O: trifluoroacetic acid = 70:29.9:0.1, v/v) was overlaid. The spectral acquisition was performed in the positive linear mode with a mass range of 20,000–50,000 Da using autoflex max MALDI–TOF. Mass spectra were smoothed, baseline-corrected for manual data processing and analyzed using Compass flexAnalysis and flexControl (version 3.4).

SEM observation. First, 20 µl of bacterial culture or spore solution or unprocessed or processed PCL films (cocultured with engineered cells) were deposited onto the sample stage. The stage was placed in a fume hood (1 h) for evaporation. The samples were treated by sputter-coating and coated with gold before the observation by SEM (Thermo Fisher, Phenom Pharos). The data were then collected and analyzed using Phenom Pharos (version 6.5.2).

Membrane fabrication. First, 6 ml of spore solution (OD ≈ 4.5) was centrifuged at 4,602*g* (to remove the supernatant) and resuspended in 2 ml of toluene. PCL pellets were dissolved in toluene (w/w, 18.5:100) at room temperature with stirring (600 r.p.m.). Then, 2 ml of spore solution (in toluene) was added to 100 ml of PCL solution and the mixture was shaken violently until the spores were well dispersed. A 6-inch clean monocrystalline silicon wafer was placed in a suitably sized glass Petri dish. Finally, 25 ml of the mixture (prepared as above) was poured over a monocrystalline silicon wafer and the system (with the lid) was placed at room temperature until the toluene was evaporated.

Characterization of mechanical properties. The films were cut by a laser cutting machine (Shanghai Diaotu Industrial). The model of the cutting sample was drawn by AutoCAD. Samples were cut into specific shapes according to the American Society for Testing and Materials (ASTM) D-638 standard. The samples were tested by a tensile testing machine (Shimadzu, AG-X plus) with a 5-kN sensor and 10 mm min^{-1} as the testing speed.

DSC measurement. All samples (3D-printed plastics or solvent-casting films) were cut into small pieces (12 mg) and placed in a crucible plate. The sample was heated at 10 °C min^{-1} from 27 °C to 120 °C (Waters, TA Q600). To eliminate the heat history, all testing groups were set to run two turns from 27 °C to 120 °C and the data were analyzed for the second heating process.

3D printing of PCL. The nozzle temperature of the 3D printer (Regenovo Biotechnology, Bio-Architect WS) was set to 120 °C to melt the evenly mixed engineered spores (1 ml, OD ≈ 4.5) and PCL (2.5 g). Before extrusion, the mixture was held inside the printer for 10 min (to melt the PCL pellets completely) before being printed onto the cooling plate (temperature, 16 °C; extrusion speed, 3 mm s^{-1}). The size of the designed object was set as 4 cm × 0.2 cm × 0.4 mm (length × width × height).

Induced degradation of living films or 3D-printed living plastics. CA-lipase (Sigma-Aldrich, CAS no. 9001-62-1) powder was dissolved in deionized water to prepare a 1 mg ml^{-1} CA-lipase solution. Living films or 3D-printed living plastics (one hairpin-shaped piece shown in Fig. 5a) were immersed in 4 ml of LB medium. Then, 0.4 ml of CA-lipase solution was added to the system to erode the living materials and release the spores. The system was placed in a shaking incubator (temperature, 37 °C; shaking speed, 220 r.p.m.) until the turbidity of the culture solution increased, indicating that the spores were successfully released from the plastics. Xylose (5 mg ml^{-1}) was supplemented to induce the expression and secretion of BC-lipase. The system was placed in a shaking incubator (temperature, 37 °C; shaking speed, 220 r.p.m.) to degrade living plastics.

Degraded plastic filtration and collection. After the degradation process, the system was filtrated by three layers of filter paper (Fuyang Beimu Paper; pore size ≈ 20–25 µm). The remaining plastics were washed three times with deionized water and then transferred into a glass bottle for further analysis.

GPC measurement. All the materials were degraded for different durations. Then, the remaining plastic debris and solution-phase byproducts were dried overnight, collected and dissolved in DMF to prepare the sample solution (concentration ≈ 1–2 mg ml^{-1}, filtered through a Teflon membrane). Then, 10 µl of solution of each sample was injected for GPC measurement on an Agilent 1260 Infinity II system equipped with an Agilent PL1113-6500 PolyPore column (7.5 mm × 300 mm) and a refractive index (RI) detector (calibrated by a poly(styrene) standard). The column was eluted with DMF at 55 °C with a flow rate of 1 ml min^{-1}. OpenLab CDS Acquisition (version 2.5) was used for data collection and analysis.

Depolymerization extent analysis. We used GPC to assess the molar mass of measured materials. GPC (Agilent 1260 Infinity II) was equipped with an autosampler (1260 Vialsampler), RI detector (1260 RID) and guard column (InfinityLab PolyPore guard column, PL1113-1500; 7.5 mm × 50 mm), followed by two PolyPore columns (InfinityLab PolyPore, PL1113-6500; 7.5 mm × 300 mm). DMF + 0.1% LiBr (w/w) was used as the eluent at 55 °C, at a flow rate of 1 ml min^{-1}. The average molar mass of the target peak (detection time ranging from 10.5 to 20.5 min) was calibrated by a poly(methyl methacrylate) standard (M_w ranging from 500 to 1,500,000 g mol^{-1}) with a narrow molar mass distribution[36]. We first calculated the molar mass of each peak (M_i) on the basis of the calibrated standards. Then, we derived the M_w of the measured samples using the following equation, where i indicates the peak number and n_i represents the percentage of area for peak i in terms of total areas.

$$M_w = \frac{\sum n_i M_i^2}{\sum n_i M_i}$$

During the disintegration process, we tracked the weight loss of each sample. The residual materials were gathered on different days and used to quantify the M_w on the basis of the GPC measurement (described above). The molar mass of the fully disintegrated materials was considered to be 132 g mol^{-1} ($C_6H_{12}O_3$). We then computed the M_w of the samples (during the disintegration process) using the following equation:

$$M_{\text{wsample}} = \frac{M_w m_t + 132(m_0 - m_t)}{m_0}$$

M_w was measured by GPC; m_t represents the weight of degraded sample after t days and m_0 represents the initial weight.

LC–MS analysis. All the materials (equivalent weight at the initial) were degraded for 7 days. The samples were mixed with pure methanol (Shanghai Lingfeng Chemical Reagent, CAS no. 67-56-1) at 1:1 (v/v). The mixtures were vortexed for 2 min and centrifuged at 3,550*g* for 10 min. The supernatant was aspirated and filtered through a 0.22-µm filter membrane (Merck Millipore). The filtered supernatant was added to an ultrafiltration tube (3 kDa; Amicon Ultra-15, UFC9003) and the tube was centrifuged at 3,550*g* for 15 min to collect the filtered liquid for future analysis.

An ultrahigh-pressure LC–MS system equipped with a Jet Stream Technology electrospray ion source (1290-6470, Agilent Technologies) was used to analyze the extracts. A Poroshell 120 EC-C18 analytical column (3 mm × 100 mm, 2.7 µm; Agilent Technologies) was used for the separation. Samples were eluted with solvent A (water with 0.1% formic acid) and solvent B (acetonitrile with 0.1% formic acid) using the following gradient program at a flow rate of 0.3 ml min^{-1}. The elution process was divided into three steps related to time, from 0 to 5 min, 5 to 40 min and 40 to 50 min. The concentration of solvent B corresponding to each elution time was 5%, 5–50% and 50–100%. The concentration of solvent B was increased linearly during each program of the elution process. The injected volume was 5 µl and the column temperature was set at 38 °C. The sheath gas flow and temperature were set at 11 ml min^{-1} and 250 °C, respectively, and the nebulizer gas temperature was set at 350 °C. The pressure of the nebulizer was 45 psi and the capillary voltage was set at 3,500 V for the positive ionization mode. Scan mode was selected for sample analysis. An Agilent MassHunter Workstation (version 10.0) was used for data collection and analysis.

The procedure of degradation by ASTM compost method. We first submitted our living films (PCL films containing the engineered spores) to a professional testing agency (SGS-CSTC Standards Technical Services). The agency used a standard composting protocol (ASTM D-5338) to evaluate the degradability of the living PCL films. Nothing else was added to the experiment and the composting facilities were closed for 45 days (no pictures were taken in between) according to the requirements of the testing agency (Supplementary Fig. 11).

We also conducted a homemade compost experiment. The compost soil was provided by a local composting facility (Evergreen Resort). Soil was first dried at 50 °C in an oven overnight and then mixed with deionized water to attain a moisture content of ~50%, consistent with the ASTM D-5338 standard. The treated soil was stored in a glass container at room temperature for 2 days before composting. The regular PCL and living PCL films were buried separately in glass containers in the as-prepared composting soil. All containers were placed in an illuminating incubator (GXM-508-4, Ningbo JIANGNAN Instrument) with 12 h of illumination and 12 h of darkness to imitate local environment conditions (temperature, 40 °C). Then, 50 ml of deionized water containing 5 mg ml^{-1} xylose was supplemented to each composting group every 4 days to ensure the soil moisture was consistent with the ASTM standard during the testing procedure. Data in Fig. 4j and Supplementary Fig. 13 were collected from December to January, while data in Supplementary Figs. 14 and 15 were collected from August to September.

Synthesis of PCL oligomer (CL-4). We first synthesized 6-hydroxyhexanoic acid (CL-1). Then, a 150-ml round-bottom flask was charged with ε-caprolactone (Aladdin; 5 g, 43.86 mol), H_2O (75 mL) and NaOH (1.84 g, 46.05 mol). The reaction was performed at room temperature overnight. After adjusting the pH of the reaction solution to 2.0 using an HCl aqueous solution (1 M), the reaction solution was extracted with ethyl acetate (4× 50 mL). The organic layer was dried over with anhydrous $MgSO_4$ and concentrated for the subsequent synthesis of CL-4.

We continued to polymerize CL using a typical procedure[37]. CL-1 (1.14 g, 10.0 mmol) and H_2O (45 µL, 2.5 mmol) were placed in a flamed, nitrogen-purged round-bottom flask equipped with a magnetic stirrer. The flask was placed in an oil bath at 80 °C and DBU (Aladdin; 13.80 mg, 0.1 mmol) was added under an argon atmosphere to start the polymerization. The reaction was quenched by adding a few drops of acetic acid and methanol mixed solution (volume ratio, 1:9) after 4 h. Then, 2 ml of CH_2Cl_2 was used to dissolve the product and the solution was precipitated into a substantial excess of diethyl ether to derive the PCL oligomer. ^{1}H nuclear magnetic resonance (400 MHz, $CDCl_3$), δ (ppm): 4.05 (t, 2H), 2.31 (t, 2H), 1.53–1.69 (m, 4H) and 1.22–1.45 (m, 2H).

3D printing of PBAT. We weighed 2.5 g of PBAT pellets and mixed them with 1.0 ml ($OD_{600} \approx 4.5$) of *B. subtilis* 164s-T7 spores carrying GFP plasmid. The nozzle temperature of the 3D printer (Regenovo Biotechnology, Bio-Architect WS) was set to 200 °C to melt the mixture of engineered spores and PBAT. Before extrusion, the mixture was held inside the printer for 15 min (to melt the PBAT pellets completely) before being printed onto the cooling plate (temperature, 16 °C; extrusion speed, 10 mm s^{-1}; extrusion pressure, 0.15 MPa). The size of the designed object was set as 3.2 cm × 0.4 cm × 0.4 mm (length × width × height).

3D printing of PBS. We weighed 2.5 g of PBS pellets and mixed them with 1.0 ml (OD600 ≈ 4.5) of *B. subtilis* 164s-T7 spores carrying GFP plasmid. The nozzle temperature of the 3D printer (Regenovo Biotechnology, Bio-Architect WS) was set to 180 °C to melt the evenly mixed engineered spores and PBS. Before extrusion, the mixture was held inside the printer for 15 min (to melt the PBS pellets completely) before being printed onto the cooling plate (temperature, 16 °C; extrusion speed, 5 mm s^{-1}; extrusion pressure, 0.1 MPa). The size of the designed object was set as 3.2 cm × 0.4 cm × 0.4 mm (length × width × height).

PLA 3D printing. We weighed 2.5 g of PLA pellets and mixed them with 1.0 ml ($OD_{600} \approx 4.5$) of *B. subtilis* 164s-T7 spores carrying GFP plasmid. The nozzle temperature of the 3D printer (Regenovo Biotechnology, Bio-Architect WS) was set to 220 °C to melt the mixture of engineered spores and PLA. The mixture was held inside the printer for 15 min (to melt the PLA pellets completely). Then, the nozzle temperature was set to 150 °C (to control the printing appearance) and the mixture was printed onto the cooling plate (temperature, 16 °C; extrusion speed, 5 mm s^{-1}; extrusion pressure, 0.3 MPa). The size of the designed object was set as 3.2 cm × 0.4 cm × 0.4 mm (length × width × height).

PHA 3D printing. We weighed 2.5 g of PHA pellets and mixed them with 1.0 ml ($OD_{600} \approx 4.5$) of *B. subtilis* 164s-T7 spores carrying GFP plasmid. The nozzle temperature of the 3D printer (Regenovo Biotechnology, Bio-Architect WS) was set to 170 °C to melt the evenly mixed engineered spores and PHA. The mixture was held inside the printer for 15 min (to melt the PHA pellets completely). Then, the nozzle temperature was set to 150 °C (to control the printing appearance) and the mixture was printed onto the cooling plate (temperature, 16 °C; extrusion speed, 5 mm s^{-1}; extrusion pressure, 0.15 MPa). The size of the designed object was set as 3.2 cm × 0.4 cm × 0.4 mm (length × width × height).

Single-screw extruder manufacturing. The temperatures of four zones in the single-screw extruder (Thermo Fisher, HAAKE PolyLab Rheomex 19/25 OS 567-2020) were set as 60 °C, 120 °C, 105 °C and 95 °C. The extrusion speed was set to 80 r.p.m. Then, 15 ml of spores ($OD_{600} \approx 18$) carrying the BC-lipase expression circuit were mixed with 500 g of PCL pellets by shaking. When the temperatures of the four zones were stable, the mixture was added to the single-screw extruder for processing. Living PCL plastics were extruded onto a conveyor to control their thickness and transported into a water bath to stabilize their shape.

Fabrication of living PET plastics. We weighed 2.5 g of PET pellets and mixed them with 1.0 ml (OD_{600} ≈ 4.5) of *B. subtilis* 164s-T7 spores carrying GFP plasmid. The mixture was well mixed by shaking and added to a high-temperature heating magnetic stirrer (IKA C-MAG HS 7), which was heated to 300 °C. The mixture was covered by a metal lid and heated for 20 min to melt the PET pellets.

Grinding or heating to release the spores. A mortar and pestle (HS-science, HS12450100) were placed in an ultraclean bench with ultraviolet irradiation (overnight) for sterilization. Then, 0.23 g of living materials carrying the engineered spores were placed in the mortar for grinding. After destruction of the materials, the mortar was supplemented with 16 ml of LB medium containing 10 μg ml^{-1} chloramphenicol. The system was well mixed and transferred into test tubes for 12 h of culturing and another 12 h of induction for GFP expression. Then, the cell cultures were centrifuged at 1,503*g* for 15 min to sediment the cells. The bacterial pellets were placed under an illuminator (Kylin-Bell, GL-1000) to verify the expression of GFP.

To release the spores by heating, we boiled the LB medium in a microwave oven and placed a piece of living PCL materials inside the heated LB medium. When the medium cooled down, we supplemented 10 μg ml^{-1} chloramphenicol and placed the system in a shaker for 12 h of culturing and another 12 h of induction for GFP expression. Then, the cell cultures were centrifuged at 1,503*g* for 15 min to sediment the cells. The bacterial pellets were placed under an illuminator (Kylin-Bell, GL-1000) to verify the expression of GFP.

Evaluation of plasmid persistence. We evaluated the maintenance of the plasmid and the functional gene. To explore the long-term persistence of the plasmid in the absence of selection for plasmid maintenance, we picked a single colony from the resistance-containing plate. We inoculated it into 3 ml of low-nutrient medium (tenfold diluted LB, to simulate the soil environment)[38]. The cell culture was incubated at 37 °C with constant shaking and diluted into the same volume of fresh medium (1:150) every day. To quantify the cells still carrying the plasmid, we plated the cell culture onto the antibiotic-containing plate and counted the CFUs (colony-forming units). To verify whether the resistance-containing cells also carried the BC-lipase gene, we randomly picked up ten clones from the antibiotic-containing plates and amplified the target fragment. The cells were considered to maintain the engineered function if the target bands appeared by DNA agarose gel electrophoresis.

Evaluation of cell growth and protein expression at elevated temperature. A single colony of *B. subtilis* was inoculated in 3 ml of LB medium containing antibiotics and cultured overnight at 37 °C (shaking speed, 220 r.p.m.). Then, we diluted the calibrated cultures (1:100) into LB medium with antibiotics. The diluted cultures (200 μl) were aliquoted into 96-well plates and then sealed with 50 μl of mineral oil to prevent evaporation. The system was incubated at 50 °C to track the OD_{600} of cultures using a plate reader (BioTek Epoch 2).

To evaluate the temperature effect on the protein expression, cells were pregrown in LB medium with the appropriate antibiotics overnight. Then, 20 μl of overnight culture was inoculated into 3 ml of LB medium at 37 °C or 50 °C for 24 h. Next, 5 mg ml^{-1} xylose was used to induce the protein expression. The culture was diluted tenfold using sterilized water. Then, a 200-μl sample was analyzed by a plate reader (BioTek Synergy H1), with the excitation at 480 nm and the emission at 520 nm. The measured value was first corrected by subtracting the blank and then divided by the corresponding OD to obtain the data.

Reporting summary

Further information on research design is available in the Nature Portfolio Reporting Summary linked to this article.

Data availability

The data processed for figure generation in this study are available within the paper and the Supplementary Information. Any additional information is available upon request. Source data are provided with this paper.

Code availability

No new code was generated for this study.

References

36. Li, Z. et al. Aggregation-induced emission luminogen catalyzed photocontrolled reversible addition–fragmentation chain transfer polymerization in an aqueous environment. *Macromolecules* **55**, 2904–2910 (2022).
37. Takizawa, K., Tang, C. & Hawker, C. J. Molecularly defined caprolactone oligomers and polymers: synthesis and characterization. *J. Am. Chem. Soc.* **130**, 1718–1726 (2008).
38. Fleming, G. T. & Patching, J. W. Plasmid instability in an industrial strain of *Bacillus subtilis* grown in chemostat culture. *J. Appl. Microbiol.* **13**, 106–111 (1994).

Acknowledgements

We thank B. An and J. Sun for providing the chassis strain and assisting with spore engineering. We thank P. Chen, T. Meng, J. Yi and J. Yan from the Nano and Advanced Materials Institute Limited (Hong Kong, China) for providing technical support and facilities for the single-screw extruder manufacturing experiment. We thank J. Xu for his assistance in synthesizing CL-4. We thank J. Zhang for her assistance in the experimental setup. This study was partially supported by the National Key Research and Development Program of China (2020YFA0908100 to Z.D.), the National Natural Science Foundation of China (3222047 and 32071427 to Z.D.; 32101185 to J.L.), the Guangdong Natural Science Funds for Distinguished Young Scholars (2022B1515020077 to Z.D.) and the Shenzhen Science and Technology Program (ZDSYS20220606100606013 and KQTD20180413181837372 to Z.D.). We are grateful to the Shenzhen Infrastructure for Synthetic Biology for providing instrument support and technical assistance.

Author contributions

C.T., Lin Wang and J. Sun designed and performed the experiments, interpreted the results and revised the paper. G.C., J. Shen and Liang Wang performed the experiments. Y.H., J.L., Z.L., P.Z. and S.Z. assisted in experimental setup, revision and data interpretation. D.Q., J.G. and J.L. assisted in research design and experimental setup. Z.D. conceptualized the research, designed the experiments, interpreted the results and wrote the paper.

Competing interests

The authors declare no competing interests.

Additional information

Supplementary information The online version contains supplementary material available at https://doi.org/10.1038/s41589-024-01713-2.

Correspondence and requests for materials should be addressed to Zhuojun Dai.

Peer review information *Nature Chemical Biology* thanks David Karig and the other, anonymous, reviewer(s) for their contribution to the peer review of this work.

nature portfolio

Corresponding author(s): Zhuojun Dai

Last updated by author(s): Jul 8, 2024

Reporting Summary

Nature Portfolio wishes to improve the reproducibility of the work that we publish. This form provides structure for consistency and transparency in reporting. For further information on Nature Portfolio policies, see our Editorial Policies and the Editorial Policy Checklist.

Statistics

For all statistical analyses, confirm that the following items are present in the figure legend, table legend, main text, or Methods section.

n/a	Confirmed
☐	☒ The exact sample size (*n*) for each experimental group/condition, given as a discrete number and unit of measurement
☐	☒ A statement on whether measurements were taken from distinct samples or whether the same sample was measured repeatedly
☐	☒ The statistical test(s) used AND whether they are one- or two-sided *Only common tests should be described solely by name; describe more complex techniques in the Methods section.*
☒	☐ A description of all covariates tested
☒	☐ A description of any assumptions or corrections, such as tests of normality and adjustment for multiple comparisons
☐	☒ A full description of the statistical parameters including central tendency (e.g. means) or other basic estimates (e.g. regression coefficient) AND variation (e.g. standard deviation) or associated estimates of uncertainty (e.g. confidence intervals)
☐	☒ For null hypothesis testing, the test statistic (e.g. *F*, *t*, *r*) with confidence intervals, effect sizes, degrees of freedom and *P* value noted *Give P values as exact values whenever suitable.*
☒	☐ For Bayesian analysis, information on the choice of priors and Markov chain Monte Carlo settings
☒	☐ For hierarchical and complex designs, identification of the appropriate level for tests and full reporting of outcomes
☒	☐ Estimates of effect sizes (e.g. Cohen's *d*, Pearson's *r*), indicating how they were calculated

Our web collection on statistics for biologists contains articles on many of the points above.

Software and code

Policy information about availability of computer code

Data collection	The i-control 2.0 software was used for collecting absorbance and fluorescence data with the Infinite 200 pro multimode reader (TECAN). Gen5 CHS software (version 3.08) was used for collecting absorbance and fluorescence data with Biotek Synergy H1 and Biotek Epoch 2. Image lab 6.0 software (version 6.0) was used for collecting SDS-PAGE with the Molecular Imager Gel Doc XR+ system (BIO-RAD). NIS-Elements AR (version 5.20.00) was used for collecting microscopic and fluorescence images with Nikon-Ti2-E. The phenom UI software (Phenom Pharos 6.5.2) was used for collecting SEM data with Phenom Pharos Desktop SEM. Compass flexAnalysis and flexControl (version 3.4) was used for data collection and analysis in MALDI-TOF (Bruker Daltonics, Billerica, MA). CytExpert (2.5.0.77) and FlowJo (v10.6.2) were used for data collection and analysis in flow cytometry. Agilent MassHunter Workstation (version 10.0) was used for data collection and analysis in LC-MS (1290-6470, Agilent Technologies, Santa Clara, CA, USA). OpenLab CDS Acquisition (version 2.5) was used in data collection and analysis in GPC (Agilent 1260 Infinity II).
Data analysis	Imaging data analysis was performed using Image J 152-win-java8. Microsoft Excel (2013) was used for plot generation and statistical analysis.

For manuscripts utilizing custom algorithms or software that are central to the research but not yet described in published literature, software must be made available to editors and reviewers. We strongly encourage code deposition in a community repository (e.g. GitHub). See the Nature Portfolio guidelines for submitting code & software for further information.

Data

Policy information about availability of data

All manuscripts must include a data availability statement. This statement should provide the following information, where applicable:

- Accession codes, unique identifiers, or web links for publicly available datasets
- A description of any restrictions on data availability
- For clinical datasets or third party data, please ensure that the statement adheres to our policy

The authors declare that the source data processed for figures generation in this study are available within the paper and its supplementary files.

Human research participants

Policy information about studies involving human research participants and Sex and Gender in Research.

Reporting on sex and gender	Not applicable
Population characteristics	Not applicable
Recruitment	Not applicable
Ethics oversight	Not applicable

Note that full information on the approval of the study protocol must also be provided in the manuscript.

Field-specific reporting

Please select the one below that is the best fit for your research. If you are not sure, read the appropriate sections before making your selection.

☒ Life sciences ☐ Behavioural & social sciences ☐ Ecological, evolutionary & environmental sciences

For a reference copy of the document with all sections, see nature.com/documents/nr-reporting-summary-flat.pdf

Life sciences study design

All studies must disclose on these points even when the disclosure is negative.

Sample size	The experiments (when replicates were shown) were performed with 3 biologically independent samples. The sample sizes were chosen based on the scale of the project and consistency with other similar published studies(Nature (2020), 580: 216–219). No sample size calculation was performed. Our results suggested that the sample sizes we chose were sufficient to test the theoretical predictions.
Data exclusions	No data were excluded.
Replication	Each experiment was repeated at least three times with similar results, suggesting the robustness of our conclusions.
Randomization	Randomization was not necessary because no allocation of the samples into experimental group was required. In our experimental set ups, regular and living materials were compared under well-controlled condition.
Blinding	Investigators were not blinded. Knowledge of a samples identity did not affect the experimental conclusion since the data were quantitative and included appropriate controls.

Reporting for specific materials, systems and methods

We require information from authors about some types of materials, experimental systems and methods used in many studies. Here, indicate whether each material, system or method listed is relevant to your study. If you are not sure if a list item applies to your research, read the appropriate section before selecting a response.

Materials & experimental systems

n/a	Involved in the study
☒	☐ Antibodies
☒	☐ Eukaryotic cell lines
☒	☐ Palaeontology and archaeology
☒	☐ Animals and other organisms
☒	☐ Clinical data
☒	☐ Dual use research of concern

Methods

n/a	Involved in the study
☒	☐ ChIP-seq
☐	☒ Flow cytometry
☒	☐ MRI-based neuroimaging

Flow Cytometry

Plots

Confirm that:

☒ The axis labels state the marker and fluorochrome used (e.g. CD4-FITC).

☒ The axis scales are clearly visible. Include numbers along axes only for bottom left plot of group (a 'group' is an analysis of identical markers).

☒ All plots are contour plots with outliers or pseudocolor plots.

☒ A numerical value for number of cells or percentage (with statistics) is provided.

Methodology

Sample preparation	Bacillus subtilis cells were diluted to appropriate density with PBS solution.
Instrument	Beckman Coulter CytoFLEX S based on CytExpert (2.5.0.77) software.
Software	CytExpert sofeware for collection and FlowJo (v10.6.2) for data analysis.
Cell population abundance	Samples contained 10,000 or more cells.
Gating strategy	We used FlowJo software's auto-gate function to acquire the target events, and then determine the fluorescent events by FITC-H≥9.0 kV.

☒ Tick this box to confirm that a figure exemplifying the gating strategy is provided in the Supplementary Information.